

SOME PROPERTIES OF THE  $\psi(3.7)$  RESONANCE, AND FEATURES OF THE TOTAL HADRONIC  
CROSS SECTION IN  $e^+e^-$  ANNIHILATION FROM 2.4 GeV TO 5.0 GeV C.M. ENERGY\*

Presented by J. A. Kadyk  
Lawrence Berkeley Laboratory  
University of California, Berkeley, California 94720

G. S. Abrams, D. D. Briggs, W. Chinowsky, C. E. Friedberg,  
G. Goldhaber, R. J. Hollebeek, A. Litke, B. A. Lulu, F. Pierre,  
B. Sadoulet, G. H. Trilling, J. S. Whitaker, J. E. Wiss, J. E. Zipse

Lawrence Berkeley Laboratory and Department of Physics  
University of California, Berkeley, California 94720

and

M. Breidenbach  
J.-E. Augustin, A. M. Boyarski, P. Bulos, J. T. Dakin, G. J. Feldman,  
G. E. Fischer, D. Fryberger, G. Hanson, B. Jean-Marie, R. R. Larsen,  
V. Luth, H. Lynch, D. Lyon, C. C. Morehouse, J. M. Paterson, M. L. Perl,  
B. Richter, B. Rapidis, R. F. Schwitters, W. Tanenbaum, F. Vannucci

Stanford Linear Accelerator Center  
Stanford University, Stanford, California 94305

ABSTRACT

An analysis of data at the  $\psi(3.7)$  resonance gives a partial width to electrons,  $\Gamma_e = 2.2 \pm 0.5$  keV, and limits on total width  $200 \text{ keV} < \Gamma < 800 \text{ keV}$ . The decay  $\psi(3.7) \rightarrow \psi(3.1)\pi^+\pi^-$  is observed with a branching ratio  $0.31 \pm 0.04$ , and  $\psi(3.7) \rightarrow \psi(3.1) + \text{anything}$  has a branching ratio of  $0.54 \pm 0.08$ . The  $\psi$  resonances appear to have the same G-parity.

An enhancement occurs in the total hadronic cross section at a c.m. energy of about 4.1 GeV, rising to about  $32 \text{ nb}$  from a level of  $15 \text{ nb}$  adjacent to peak, which is about  $300 \text{ MeV}$  wide. The integrated cross section for the peak is about  $5.5 \text{ nb-GeV}$ , comparable to that for the  $\psi(3.7)$  and  $\psi(3.1)$  resonances.

Une analyse des mesures expérimentales sur la résonance  $\psi(3.7)$  donne une largeur partielle pour la désintégration en une paire d'électrons,  $\Gamma_e = 2.2 \pm 0.5 \text{ keV}$ , et des limites sur la largeur totale,  $200 \text{ keV} < \Gamma < 800 \text{ keV}$ . La désintégration  $\psi(3.7) \rightarrow \psi(3.1)\pi^+\pi^-$  est observée avec un rapport d'embranchement de  $0.31 \pm 0.04$ , et  $\psi(3.7) \rightarrow \psi(3.1) + \text{n'importe quoi}$  a un rapport d'embranchement de  $0.54 \pm 0.08$ . Les résonances  $\psi$  semblent avoir la même parité G.

Une hausse de la section efficace totale hadronique se produit à une énergie dans le centre de masse de 4.1 GeV. La section efficace monte de son niveau de  $15 \text{ nb}$  à des énergies avoisinantes jusqu'à  $32 \text{ nb}$  avec une largeur d'à peu près  $300 \text{ MeV}$ . L'intégrale de la section efficace pour cette structure est approximativement  $5.5 \text{ nb-GeV}$ , comparable à celles des résonances  $\psi(3.7)$  et  $\psi(3.1)$ .

MASTER

\*Work supported by the U. S. Atomic Energy Commission.

NOTICE

This report was prepared as an account of work sponsored by the United States Government. Neither the United States nor the United States Energy Research and Development Administration, nor any of their employees, nor any of their contractors, subcontractors, or their employees, makes any warranty, express or implied, or assumes any legal liability or responsibility for the accuracy, completeness or usefulness of any information, apparatus, product or process disclosed, or represents that its use would not infringe privately owned rights.

I.  $\psi(3.7)$ 

Following the discovery of the  $\psi(3.1)$ , a systematic search was initiated to look for other very narrow resonances. The method of search has been described previously,<sup>1</sup> but can be briefly explained as an automatic ramping of the SPEAR beam energy by  $\sim 1$  MeV steps every few minutes, the data collected at each energy being processed on-line by the SLAC IBM 168 computer complex. By this means, the cross sections were immediately computed in very fine steps ( $\Delta E_{\text{cm}} \sim 2$  MeV) although with large statistical errors. However, this technique was more than adequate in detecting narrow resonances as was proven by going back over the  $\psi(3.1)$  resonance, which was seen clearly, and, much more importantly, by the discovery of the  $\psi(3.7)$  soon after the search began<sup>2</sup> (see Fig. 1).<sup>\*</sup> The sensitivity was such that resonances having  $\sigma_{\text{had}}$  at the peak greater than a few hundred nb would have been detected.

Shortly after observing the  $\psi'$ , the shape of the peak was carefully mapped out as illustrated in Fig. 2, in order to obtain  $\Gamma_e$  by integration of the cross section, as was done for the  $\psi$ . The result after radiative corrections is:

$$\int \sigma_{\text{had}} dW = 3.7 \pm 0.9 \text{ nb-GeV}.$$

This is about a factor of 3 less than for the  $\psi$ . To obtain the width to the  $e^+e^-$  channel and the total width, it is necessary to know the branching ratio into  $e^+e^-$ , or into  $\mu^+\mu^-$ , if  $\mu$ -e universality is assumed. First attempts to observe the leptonic modes were disappointing, only the slightest suggestion of any enhancement being visible. Soon it became clear that the situation was rather complex, since it was discovered that the  $\psi'$  decayed into the  $\psi$  part of the time,<sup>2</sup> and since the  $\psi$  subsequently decayed into leptons, that decay mode must be distinguished from those due to direct decay of the  $\psi'$ . We will return to discuss the  $\psi'$  cascade decay in a moment.

---

<sup>\*</sup>Within this paper we will subsequently refer to the  $\psi(3.7)$  as  $\psi'$  and  $\psi(3.1)$  as  $\psi$ .

Although the  $e^+e^-$  decay mode of the  $\psi'$  was difficult to separate from the dominant  $t$ -channel Bhabha background, as well as from the  $\psi$  electron decay mode, the  $\mu^+\mu^-$  mode was more easily isolated, as will be seen. Subtracting the QED background, the branching ratio to muons is found:

$$\frac{\Gamma(\psi' \rightarrow \mu^+\mu^-)}{\Gamma(\psi' \rightarrow \text{all})} \approx 0.005 \pm 0.003 .$$

If we assume  $\mu$ -e universality and the spin assignment  $J = 1$ , then the widths are determined:

$$\begin{aligned} \Gamma_e(\psi') &= 2.2 \pm 0.5 \text{ keV} , \\ 200 \text{ keV} &< \Gamma(\psi') < 500 \text{ keV} . \end{aligned}$$

The electron width determination is nearly independent of the lepton ratio, because the latter is so small, and the errors on  $\Gamma_e$  reflect just the uncertainty of  $\int \sigma_{\text{had}} dW$ . The large uncertainty in the limit on the total width comes about partly from the background subtraction, which is reflected in the  $\mu^+\mu^-$  branching ratio, but also from the possible contribution due to interference with the QED amplitude. The presence or extent of the interference has not yet been investigated in detail experimentally. The expectation is to obtain a much more precise determination of these quantities when more data is collected. The position of the peak is known more accurately than originally, due to recalibration of a flip coil used to determine the SPEAR magnetic guide field. The new value is  $3.684 \pm 0.005$  GeV. It should be noted that the  $\psi'$ , although very narrow, seems to be markedly broader than the  $\psi$ .

Let us now examine in more detail the decay

$$\psi' \rightarrow \psi \pi^+ \pi^- , \quad (1)$$

the mode by which this cascade decay was discovered. From a sample of about 30,000 events, the missing mass distribution shown in Fig. 3 was obtained, showing conclusive evidence for decay (1). The branching ratio for decay by (1) was determined, after suitable efficiency corrections and background subtraction:

$$\frac{\Gamma(\psi' \rightarrow \psi \pi^+ \pi^-)}{\Gamma(\psi' \rightarrow \text{all})} = 0.31 \pm 0.04 .$$

The branching ratio for the inclusive decay,

$$\begin{array}{l} \psi' \rightarrow \psi + X \\ \quad \downarrow \\ \quad \mu^+ \mu^- \end{array} \quad (2)$$

was also found, by isolating the muon pair decays of the  $\psi$ , and scaling by the known leptonic branching ratio of the  $\psi$ . Figure 4 shows the square of the effective  $\mu^+ \mu^-$  mass, and the events corresponding to  $\psi$  decay in (2) are clearly separated. Approximately 800 events correspond to reaction (2). Here, the highest momentum positive and negative particles have been chosen, and  $e^+ e^-$  decays have been eliminated by requiring small pulses from the shower counters. The  $e^+ e^-$  mode was not used for this purpose, due to the relatively large background from the radiative tail of the Bhabha scattering process. The result was:

$$\frac{\Gamma(\psi' \rightarrow \psi + \text{anything})}{\Gamma(\psi' \rightarrow \psi \pi^+ \pi^-)} = 1.80 \pm 0.10 .$$

We expect the "anything" above to consist, at least partly, of  $2\pi^0$ , since  $\pi^+ \pi^-$  is observed (unless the pions are in an  $I = 1$  state). The ratio above has the theoretical values 1.5, 1.0, and 3.0, for  $\pi\pi$  isospin states of 0, 1, and 2, respectively (these become 1.52, 1.00, and 3.10 for uniform phase space when the  $\pi^{\pm}/\pi^0$  mass difference is taken into account). Clearly isospin-zero is preferred, but the lack of good agreement may result from admixture of other final states.

Corresponding to the ratios presented above, there is the branching ratio of cascade decays to all  $\psi'$  decays:

$$\frac{\Gamma(\psi' \rightarrow \psi + \text{anything})}{\Gamma(\psi' \rightarrow \text{all})} = 0.54 \pm 0.08 .$$

It is of interest to look at the recoil mass against the  $\psi$  in reaction (2) as determined from the  $\mu^+ \mu^-$  decay, a relatively clean sample. As seen in Fig. 5, there is no peak at low mass indicating a decay of  $\psi'$  into a single low mass particle, such as a  $\gamma$  or  $\pi^0$ . The apparent absence of the single  $\pi^0$  cascade decay and the observed large branching ratio by two final

state pions in (1) indicates that the  $\psi$  and  $\psi'$  have the same G parity, and that G parity is, to a good approximation at least, preserved in the decay process.

A study was also made of the exclusive channel:

$$\psi' \rightarrow \psi \pi^+ \pi^- \quad (3)$$

$$\downarrow \mu^+ \mu^- \text{ or } e^+ e^- .$$

Here, a selection of the  $\psi$  leptonic modes was made, and rather loose cuts imposed by energy-momentum conservation to insure that no particles were unobserved in the 4-prong event. Figure 6 shows the very clean sample which results, a subset of Fig. 3. The ratio between these samples is in good agreement with the known leptonic decay branching ratio of the  $\psi$ , which is about 1/4. This sample, consisting of about 350 events, was used to study the final state distributions. That the decay (1) occurs predominantly through S wave is supported by the observed angular distribution for the  $2\pi$  system, which is consistent with isotropy, and the distribution of leptons from  $\psi$  decay, which is consistent with  $1 + \cos^2 \theta$  (as well as with isotropy). Furthermore, the  $\psi$  angular distribution seems consistent with isotropy.

However, the  $M(\pi^+ \pi^-)$  plot (shown in Fig. 7) shows a rather strong suppression of low mass states, and this is not due to instrumental effects investigated thus far. In particular, it is not caused by a trigger bias against the low-momentum pions, since the analysis required the trigger to be satisfied by the  $\psi$  decay leptons alone. The inclusion of final state S-wave interaction does not appear to be sufficient to explain the observed distribution. Although the isotropic angular distribution suggests S-wave, higher angular momentum states cannot be excluded, and the interpretation of this mass distribution is still open at this time.

The present data sample and results of analysis of the  $\psi'$  is summarized in Table I. The principal conclusions which may be drawn at present, are that the  $\psi(3.7)$  resembles the  $\psi(3.1)$  in being a very narrow resonance for such a large mass, and it has comparable coupling to the  $e^+ e^-$  state. However, it decays with a large branching ratio into the  $\psi$ , at a rate that

appears to be much less strongly suppressed than the direct decay into the more usual hadron final states. That this cascade decays via two pions, but not one pion, indicates that the  $\psi$  and  $\psi'$  have the same G quantum number, which appears to be odd as determined from analysis of  $\psi$  decays. The relative rates of decay of  $\psi' \rightarrow \psi$  plus charged pions or undetected particles (neutrals) in the cascade decay seems to prefer an  $I = 0$  final pion state, though this is an inference needing direct confirmation.

## II. THE TOTAL CROSS SECTION AND THE ENHANCEMENT AT 4.1 GeV

Leaving aside now the very sharp  $\psi$  resonance peaks which are the most spectacular features of the SPEAR data, we should take a careful look into the "foothills" of the cross-section plot.<sup>3</sup>

First of all, let us look in Fig. 8 at the energy dependence of  $R = \frac{\sigma_{\text{tot}}(\text{hadrons})}{\sigma_{\text{QED}}(\mu^+\mu^-)}$  on a log scale. This shows clearly the beautiful work done several years ago at Orsay in studies of the  $\rho$ ,  $\omega$  and  $\phi$ , and the "average" values from Frascati at intermediate energies, where the overabundant production of hadrons first became evident. Following at higher energies are current SPEAR results showing the generally smooth behavior of  $R$ , relatively flat to about 3.6 GeV, then an enhancement whose exact nature is not yet clear, and finally at the highest energy values observed perhaps a leveling off of  $R$ . The "bump" appears much more striking on a linear scale in Fig. 9, where there is shown both  $R$  and  $\sigma_{\text{total}}$ . The measured values are generally spaced 0.2 GeV in  $W(=\sqrt{s})$ , the c.m. energy, although some data with finer resolution, 0.1 GeV, exists in the regions of the  $\psi(3.1)$  and the 4.1 enhancement.

The prior descriptions of the sharp resonances did not discuss very much about backgrounds, corrections and other analysis details since the signal was so large as to render some of these corrections unnecessary (the non-annihilation background in the  $\psi$  region is at most about 0.1%). However, at the more civilized cross sections of 20-30 nb, the corrections are not negligible, and perhaps should be mentioned again briefly to present a

complete picture. The trigger requires at least two charged tracks within the  $0.65(4\pi)$  sensitive solid angle coverage, where the efficiency for each track is well above 90% for high momentum tracks, but drops rapidly for momenta below 200 MeV/c. As described in the earlier paper, a hadron event was defined as having  $\geq 3$  tracks, or two tracks acoplanar by more than  $20^\circ$  with small pulse height (not electrons). These observed efficiencies and acceptances are incorporated in a Monte-Carlo program used to compute the average efficiencies per event as a function of number of charged particles. From these the true multiplicities were derived through a set of simultaneous equations, and the average detection efficiency,  $\bar{\epsilon}$ , also determined. It should be noted that these determinations use a model by which the Monte-Carlo events are generated, but the form of the model does not enter directly into the determination of  $\bar{\epsilon}$ . That  $\bar{\epsilon}$  is quite insensitive to the model was verified by using three quite different models (including a jet model) which predicted values for  $\bar{\epsilon}$  differing by only  $\pm 5\%$ .

Background due to beam gas interactions was determined from the longitudinal distributions of reconstructed vertices, which peak strongly in the interaction region. The subtraction for this background was  $< 8\%$  at all energies. The contamination from photon-photon processes was measured using small-angle electron tagging counters (20  $\mu\text{rad}$ ), and was appreciable only in the two-prong events, varying between 8% and 3% from highest to lowest energies. For  $\geq 3$  prongs, this type of contamination was  $\leq 2\%$ .

The radiative tails due to the  $\psi(3.1)$  and  $\psi(3.7)$  were removed, and then the resulting cross-section values corrected for the nonresonant radiative effects.

The normalization for  $\sigma_{\text{total}}$  was the sample of Bhabha events collected concurrently, the validity of QED having been previously established in this energy range (except, of course, for the resonances).<sup>5</sup>

Aside from these corrections, an estimated point-to-point systematic uncertainty of 8% has been combined quadratically. Additional slowly varying systematic variations not included might exist at the 10%-15% level, as

well as an uncertainty in absolute normalization of about 10%.

The principal structure seen in Fig. 9 is the peak at about 4.1 GeV, having a width of 250-300 MeV, and rising from a level of  $\sim 18$  nb outside the peak to  $\sim 32$  nb at the top. The integrated total cross section corresponding to the peak is about 5.5 nb-GeV, a value comparable to that of the  $\psi$  and  $\psi'$ . At present there is very little data available in the region of the 4.1 GeV enhancement, because cross sections in this region are relatively small, and so large amount of running has been done at this energy. Therefore, there are at the moment no significant results on decay modes from the peak region. However, a large amount of data does exist just below the peak at 3.8 GeV, and also above the peak at 4.8 GeV. Studies of this energy region are presently in progress, and no results are yet available. It is, of course, of great importance to understand this enhancement, whether as a resonance or a threshold effect, and particularly its possible relationship to the two  $\psi$  particles and the rise in R beginning at 3.6 GeV.

Table I. Preliminary Determination of Parameters of  $\psi(3.7)$  Resonance.

Quantity	Value	Comment
Mass	$3684 \pm 5$ MeV	
$\int \sigma_{had} dW$	$3.7 \pm 0.9$ $\mu\text{b-MeV}$	
Partial decay width to ee pairs, $\Gamma_e$	$2.2 \pm 0.5$ keV	Spin J = 1 assumed
Full width, $\Gamma$	$200 \text{ keV} < \Gamma < 800 \text{ keV}$	
-----		
Major Decay Modes	Branching Ratio	
$\psi(3.7) \rightarrow \psi(3.1)\pi^+\pi^-$	$0.31 \pm 0.04$	
$\psi(3.7) \rightarrow \psi(3.1) + \text{anything}$	$0.57 \pm 0.08$	
G-Parity:	Inferred to be the same as $\psi(3.1)$ due to above decay to $\psi(3.1)\pi\pi$ , and apparent absence of $\psi(3.1)\pi$ mode. No determinations yet from direct (i.e., non-cascade) decays.	
Spin:	Inferred to be $1^-$ , due to production via $e^+e^-$ annihilation. No determination yet from interference with QED amplitude.	



REFERENCES

1. A. M. Boyarski et al., Search for Narrow Resonances in  $e^+e^-$  Annihilation in the Mass Region 3.2 to 5.9 GeV, SLAC-PUB-1523 and LBL-3632. January 1975, submitted to Phys. Rev. Letters. Also, see previous talk by M. Breidenbach.
2. G. S. Abrams et al., Discovery of a Second Narrow Resonance in  $e^+e^-$  Annihilation, Phys. Rev. Letters 33, 1453 (1974).
3. G. S. Abrams et al., Observation of the Decay Modes  $\psi(3.7) \rightarrow \psi(3.1) + \text{Anything}$  and  $\psi(3.7) \rightarrow \psi(3.1)\pi^+\pi^-$ , LBL-3369, March 1975, to be submitted for publication.
4. J.-E. Augustin et al., Total Cross Section for Hadron Production by Electron-Positron Annihilation Between 2.4 GeV and 5.0 GeV Center-of-Mass Energy, SLAC-PUB-1520 and LBL-3621, January 1975, submitted to Phys. Rev. Letters.
5. J.-E. Augustin et al., Phys. Rev. Letters 34, 233 (1975); E. L. Beron et al., Phys. Rev. Letters 33, 663 (1974).

FIGURE CAPTIONS

- Fig. 1. Examples of data taken in the early scan or search mode, leading to the discovery of the  $\psi(3.7)$ . (a) Data taken in the vicinity of the  $\psi(3.1)$  to confirm the sensitivity of the method, (b) data taken during the run in which the  $\psi(3.7)$  was first found.
- Fig. 2. The  $\psi(3.7)$  resonance peak as defined by much higher luminosities per point. Some apparent fluctuations are due to a small current-dependency of the SPEAR beam energy width.
- Fig. 3. Distribution of missing mass,  $M_X$ , opposite  $\mu^+\mu^-$  in reaction (1). The peak corresponds to decays in which  $X \equiv \psi(3.1)$ .
- Fig. 4. Effective mass distribution of  $\mu^+\mu^-$  arising from  $\psi(3.7)$  decays. The muons pairs coming from  $\psi(3.1)$  decay in the cascade decay (?) are well separated.
- Fig. 5. Missing mass distribution for reaction (2). Note the absence of any peak at low mass.
- Fig. 6. Missing mass distribution similar to Fig. 3, but for the subset of events shown there which correspond to reaction (3) and in which the observed particles satisfy overall momentum-energy conservation, within measurement errors.
- Fig. 7. Effective mass distribution of the  $\pi^+\pi^-$  pair from reaction (3). The curve represents the prediction for uniform phase space corrected for detector acceptance.
- Fig. 8. Log plot of  $R = \frac{\sigma_{\text{hadrons}}}{\sigma_{\text{QED}}(\mu^+\mu^-)}$  vs total c.m. energy.
- Fig. 9. (a) The total hadronic cross section,  $\sigma_T$ , vs c.m. energy,  $W$ . (b)  $R = \sigma_T/\sigma_{\text{QED}}(\mu^+\mu^-)$  vs  $W$ . Corrections have been made for the radiative tails of the  $\psi(3.7)$  and  $\psi(3.1)$  resonances.

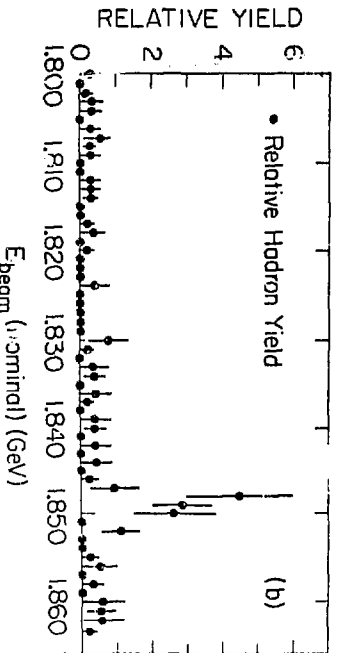
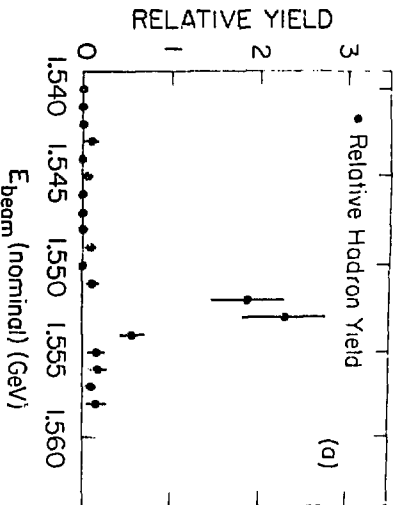


Fig. 1

XBL 733525

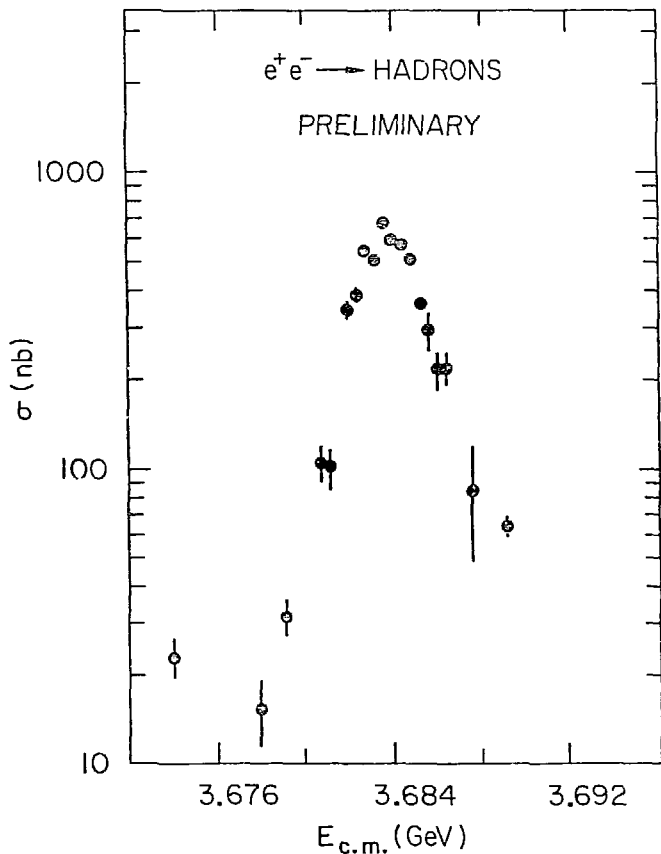
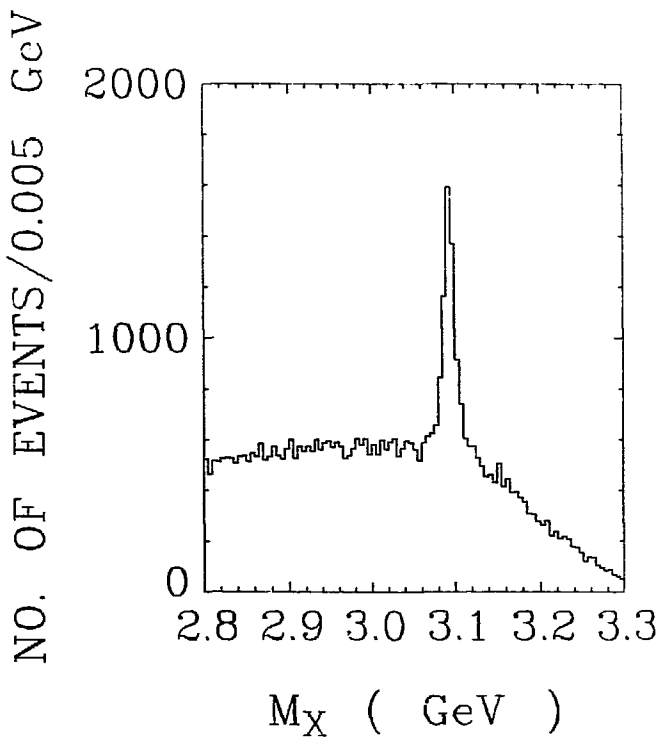


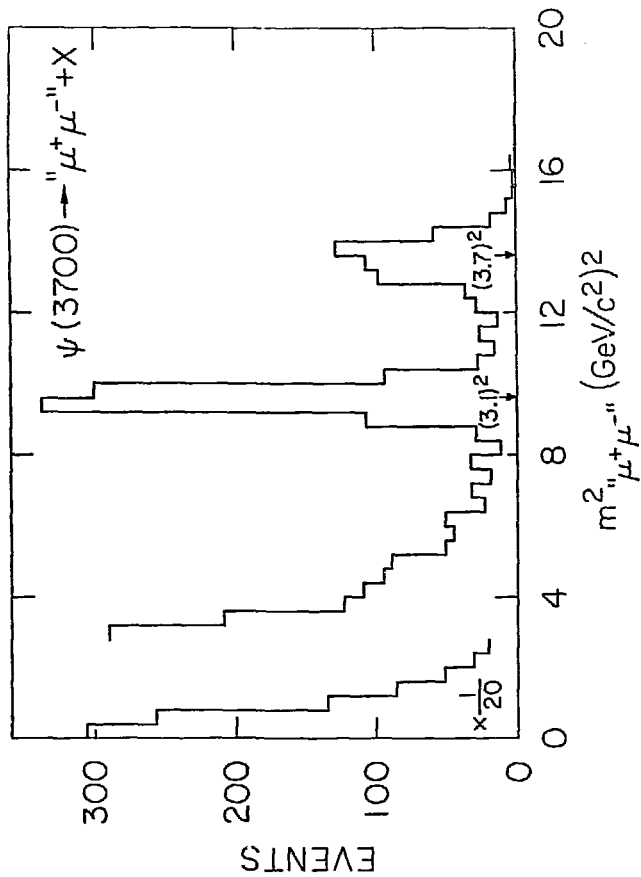
Fig. 2

XBL 753-526



NBL 753-527

Fig. 3



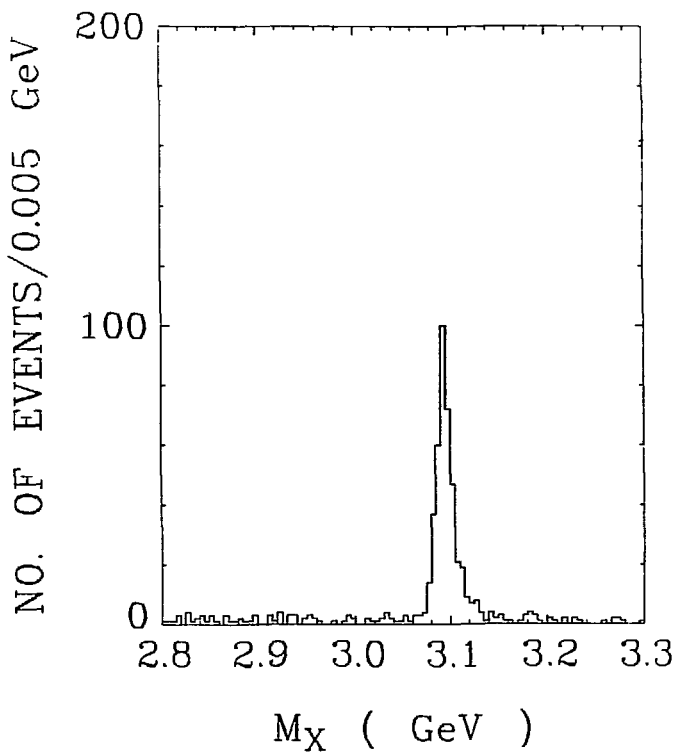
NIM. 753 528

Fig. 4

particles incident on the targets. Because the intensity of the carbon beam was so much lower than the intensity available with the other three types of beam particles, it was necessary to bring the monitor much closer to the target during this part of the experiment. As a result, the telescope was placed within six inches of the targets for the  $^{12}\text{C}$  runs. This was the minimum distance allowed by the geometry of the target box.

The monitor of course only provided a relative normalization. In order to get an absolute normalization for our cross sections we needed to know precisely the incident flux. For this purpose we used an ion chamber and a secondary emission monitor placed in the primary beam upstream of our targets. The monitor was calibrated against the ion chamber and SEM according to the procedure described in section IV below.

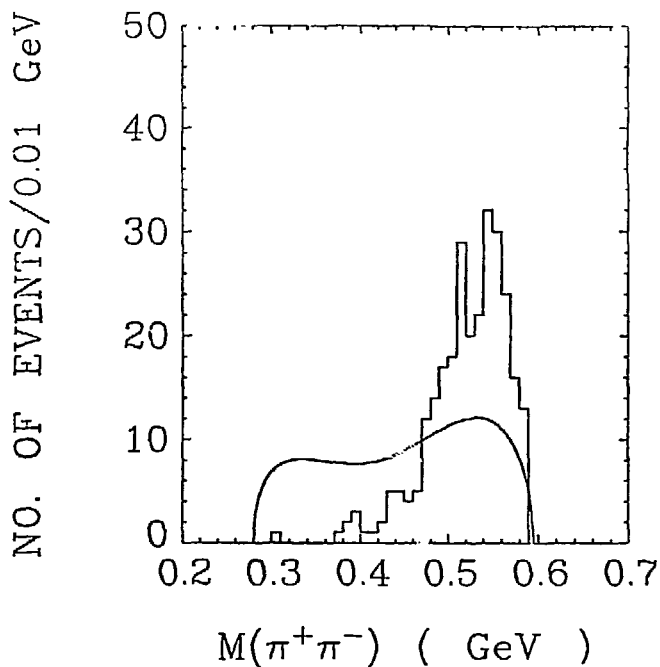
The ion chamber itself was calibrated against a pair of scintillation counters placed directly in the beam in the following way. The charge created in the ion chamber by the beam was collected and measured by an electrometer. The full scale deflection of the meter which read out the electrometer charge could be adjusted from a maximum sensitivity of  $3 \times 10^7$  up to  $10 \times 10^{10}$  incident charges per pulse. The charge produced in the ion chamber is proportional to  $Z^2$  where  $Z$  is the charge of the beam particles. When a  $^{12}\text{C}$  beam was used, the reading of the ion chamber was about 36 times the number of particles which actually passed through it.



XBL 753 530

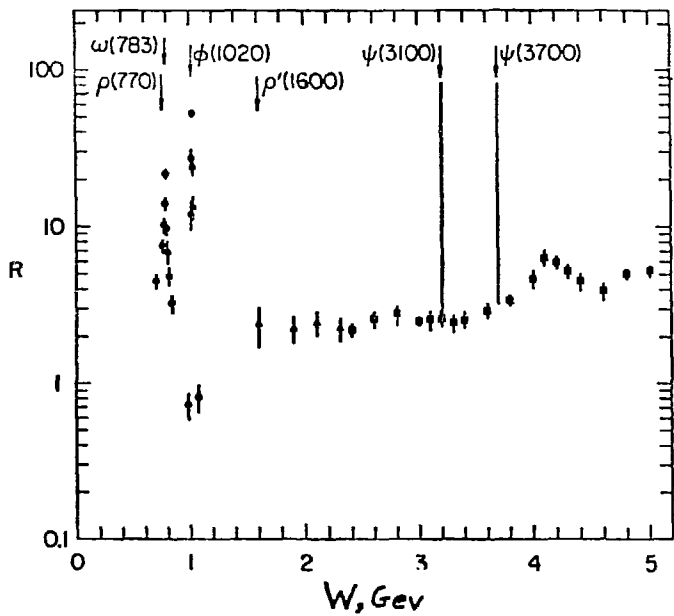
Fig. 6





XBL 733-531

Fig. 7



XBL 753-532

Fig. 8

Microscopic Models for Heavy Ion Scattering  
at Low, Intermediate and High Energies<sup>\*†</sup>

J. P. Vary and C. B. Dover

Brookhaven National Laboratory, Upton, New York 11973

ABSTRACT and SUMMARY

We trace the evolution with energy of a lowest-order microscopic model for nucleus-nucleus interactions from 10 MeV/nucleon to 1 TeV/nucleon incident energies. There are three essential questions investigated; first, what is the interaction and how carefully must we obtain its ingredients; second, what is the appropriate dynamical framework in which to employ this interaction; and third, for what processes do we expect this lowest order model to be valid. To answer the first question, we present a development of an optical potential model obtained by folding the densities of the interacting nuclei with a suitably renormalized nucleon-nucleon force. At low energies (< 50 MeV/nucleon) there is sufficient data to demonstrate marked sensitivity to the choices of density and range of the elementary force. When the densities are taken with correct asymptotic properties and the interaction has a

-----

\* Work performed under the auspices of the U.S. Atomic Energy Commission.

† Invited paper for the Second High Energy Heavy Ion Summer Study, Lawrence Berkeley Laboratory (July 15-26, 1974), presented by J. P. Vary.